Int. J. Heat Mass Transfer. Vol. 29, No. 1, pp. 95–105, 1986
Printed in Great Britain

0017-9310/86 $3.00 + 0.00
Pergamon Press Ltd.

Heat and mass transfer with condensation in laminar and turbulent boundary layers along a flat plate

F. LEGAY-DESESQUELLES and B. PRUNET-FOCH
Laboratoire d'Aérothermique du C.N.R.S., 4 ter, route des Gardes, F 92190 Meudon, France

(*Received* 10 *April* 1985)

Abstract—An experimental and numerical study of heat and mass transfer in an incompressible boundary layer with condensation over a flat plate is presented. The air–steam flow at atmospheric pressure is saturated; its velocity is smaller than 6 m s^{-1}; the Reynolds number calculated with the abscissa along the plate ranges from 10^4 to 10^5 for the laminar boundary layer and from 3×10^5 to 10^6 for the turbulent one. The temperature difference between the main flow and the cold wall does not exceed 20°C. A finite-difference method is used to calculate the velocity, temperature and concentration fields; the numerical results are in good agreement with experiments for laminar and turbulent boundary layer.

1. INTRODUCTION

CONDENSATION effect may be used in various problems, e.g. the recovery of the latent heat present in humid air to improve the efficiency of some exchangers; or the chemical extraction of a mixture component by condensation. Consequently, both heat and mass transfer are important in condensation phenomena.

The aim, then, of the present study is to evaluate heat and mass transfer at the wall when hot air saturated with steam flows along a horizontal flat plate. This plate is uniformly heated at a temperature which is slightly smaller than the main flow one. The thermal gradient which exists in the boundary layer induces steam condensation, release of latent heat and then an increase in the heat and mass exchanges.

In this paper, our attention is focused on small temperature differences and low level exchange. Experiments and numerical calculations are performed for laminar and turbulent boundary layer.

Following Nusselt (1916), Sparrow *et al.* [1] studied condensation heat transfer over an horizontal flat plate when condensation is assumed to occur only on the condensate film located at the cooled surface. The liquid film and the gaseous boundary layer were separately treated and compatibility conditions at the interface were written down. In this analysis, mass conservation equations for the noncondensable gas and the condensing vapor are used; however, no attention is paid to the relationship between the concentration and the temperature of the condensing vapor, the so-called 'saturation condition'.

If the assumptions Sparrow *et al.* adopted are correct when the relative humidity of the main flow is low (high superheat), they become approximate when the vapor is saturated because thermodynamical non-equilibrium exists in the boundary layer; so, at any point, the concentration of the condensing vapor should be larger than the saturated concentration corresponding to the temperature of this point. Moreover, when thermal equilibrium exists, the saturated part of the vapor condenses and is dispersed in the mixed gases as liquid droplets.

In their paper, Hijikata and Mori [2] applied this thermodynamical equilibrium condition to the condensation of a saturated vapor mixed with a non-condensable gas in a forced convective laminar boundary-layer flow along a cooled flat plate. Moreover, the principle of similarity for each distribution profile of velocity, temperature and concentration was assumed and, in addition, the velocity profile was a simplified polynomial of degree three.

In the present work, the 'saturation condition' is also assumed to hold everywhere; the condensation heat transfer is studied in both laminar and turbulent boundary layers; however, the distribution profiles of the variables are determined step-by-step by a finite-difference numerical method.

2. EXPERIMENTAL PROCEDURE

A mixture of hot air and steam, under saturated conditions at a temperature T_∞, flows along a flat plate uniformly heated at a temperature T_w lower than T_∞. Flow velocities are smaller than 6 m s^{-1} and temperature differences ΔT between the main flow and the wall are smaller than 20°C; T_∞ is below 100°C.

Experiments were carried out in a low-speed wind tunnel with thermally insulated walls. The production capacity of the steam generator is equal to 1500 kg h^{-1} at 6 bars. Air is heated between 40° and 60°C and mixed with steam at atmospheric pressure in order to obtain a saturated mixed fluid. The dew-point condition was controlled in the settling chamber by measuring the amount of condensed water in a given time before and during each run. The cross-section of the 0.8-m-long test chamber is rectangular (0.4 m × 0.2 m); it is bounded by two vertical glass walls which were heated to avoid undesirable condensation. The exchange

NOMENCLATURE

c_p	specific heat at constant pressure [J kg^{-1} K^{-1}]
D	diffusion coefficient [m^2 s^{-1}]
h	enthalpy [J kg^{-1}]
l	mixing length [m]
L	latent heat of condensation [J kg^{-1}]
$\dot{m}$	mass flux [kg m^{-2} s^{-1}]
Nu	Nusselt number
p_v	vapor pressure [Pa]
Pr	Prandtl number
$\dot{q}_s$, $\dot{q}_t$	heat flux, sensible or total, respectively [J m^{-2} s^{-1}]
Re_x	Reynolds number calculated with x
Sc	Schmidt number
T	temperature [K]
ΔT	temperature difference between the main flow and the wall
u, v	velocity components [m s^{-1}]
$\bar{u}$, $\bar{v}$, u', v'	mean values and fluctuations of u, v, respectively
x, y	coordinates [m].

Greek symbols

δ	boundary-layer thickness [m]
λ	thermal conductivity [W m^{-1} K^{-1}]
μ	dynamic viscosity [kg m^{-1} s^{-1}]
μ_{lam}, μ_{turb}, μ_{eff}	laminar, turbulent and effective viscosity, respectively
ρ	mass per unit volume of mixture [kg m^{-3}]
τ_w	shearing stress [kg m^{-1} s^{-2}].

Subscripts

g	non-condensable gas
l	liquid
v	vapor
w	wall
∞	main flow.

surface is the lower horizontal wall of the test chamber itself; it is heated by hot water circulation in 12 independent compartments. A fully-developed laminar boundary layer is obtained by an elliptic leading edge and an upstream suction slit. When this slit is shut, tripping wires are needed to obtain the fully-established turbulent regime for which numerical calculation is performed.

A crucial point in these experiments was the presence, on the exchange plate, of the condensate for temperature differences larger than 10°C and 1°C for laminar and turbulent boundary layers, respectively. This condensate must be eliminated in order to improve the heat transfer; several methods were simultaneously employed:

- —the plate was covered with a very thin layer of plaster (less than 0.2 mm) in order to obtain a wettable surface;
- —the flat plate was very slightly inclined to facilitate the downstream flow of the condensate;
- —two small slots filled with cotton wicks were drilled downstream on each side of the surface of the plate.

Under these conditions, the remaining liquid film had a negligible effect on the heat transfer and might not be taken into account. So, the hypothesis of the numerical calculation is verified.

As the temperature difference between the internal and external faces of the model is small, the heat flux could not be measured directly with good accuracy, at least in the laminar boundary layer. Therefore, a miniature thermocouple was used and temperature profiles were measured at various abscissae. Since, the observed and calculated temperature profiles are in good agreement, the calculated value of heat transfer at the wall was considered as being correct.

Successive experiments were performed with various wall temperatures while the fluid velocity u_∞ and the temperature T_∞ remained constant.

3. MATHEMATICAL MODEL AND NUMERICAL CALCULATION

The main assumptions necessary to establish boundary-layer equations are:

- —the liquid film which remains on the wall is so thin that it has no influence on the flow field and on the heat transfer;
- —the volume of the condensed droplets in the gaseous boundary layer is negligible; thus the classical Navier–Stokes equations are still valid;
- —there is no interaction between the droplets.

Thus, the droplets' velocity is equal to the velocity $\vec{u}$ (i.e. $u_l = u$, $v_l = v$).

With these assumptions, the conservation equations may be expressed as:

- total mass conservation:

$$\frac{\partial(\rho u)}{\partial x} + \frac{\partial(\rho v)}{\partial y} = 0 \tag{1}$$

- non-condensable gas mass conservation:

$$\frac{\partial(\rho_g u_g)}{\partial x} + \frac{\partial(\rho_g v_g)}{\partial y} = 0 \tag{2}$$

● momentum conservation:

$$\frac{\partial(\rho u^2)}{\partial x}+\frac{\partial(\rho uv)}{\partial y}=\frac{\partial}{\partial y}\left(\mu\frac{\partial u}{\partial y}\right) \tag{3}$$

● energy conservation:

$$\frac{\partial(\rho hu)}{\partial x}+\frac{\partial(\rho hv)}{\partial y}=\frac{\partial}{\partial y}\left(\lambda\frac{\partial T}{\partial y}\right) \tag{4}$$

where

$$\rho u=\rho_g u_g+\rho_v u_v+\rho_l u_l$$

$$\rho hu=\rho_g h_g u_g+\rho_v h_v u_v+\rho_l h_l u_l$$

and similarly for ρv and ρhv, with

$$h_g=c_{pg}(T-T_\infty)$$

$$h_v=c_{pv}(T-T_\infty)$$

$$h_l=c_{pl}(T-T_\infty)-L.$$

Moreover, let us assume that diffusional longitudinal velocities are small compared with u; hence,

$$u_g=u_v=u_l=u. \tag{5}$$

Fick's law for a binary mixture may be written as:

$$v_g=v-\frac{\rho_g+\rho_v}{\rho_g}D\frac{\partial}{\partial y}\left(\frac{\rho_g}{\rho_g+\rho_v}\right). \tag{6}$$

Then, equations (2) and (4) become:

$$\frac{\partial(\rho_g u)}{\partial x}+\frac{\partial(\rho_g v)}{\partial y}=\frac{\partial}{\partial y}\left[(\rho_g+\rho_v)D\frac{\partial}{\partial y}\left(\frac{\rho_g}{\rho_g+\rho_v}\right)\right] \tag{2'}$$

$$\frac{\partial(\rho hu)}{\partial x}+\frac{\partial(\rho hv)}{\partial y}=\frac{\partial}{\partial y}\left(\lambda\frac{\partial T}{\partial y}\right)+\frac{\partial}{\partial y}\left[(\rho_g+\rho_v)D(h_g-h_v)\frac{\partial}{\partial y}\left(\frac{\rho_g}{\rho_g+\rho_v}\right)\right]. \tag{4'}$$

In addition to these four conservation equations, the partial pressure p_v of the condensing vapor is related to the local temperature T in consequence of local thermodynamic equilibrium:

$$p_v=f(T).$$

From this equation and with the assumption of constant static pressure in the boundary layer, when T is known the air partial pressure and the mass concentrations of air and steam can be deduced if the two gases are assumed perfect.

Only four unknowns remain in the system: u, v, T and ρ_l. The boundary conditions are:

—at $y=0$

$$\left.\begin{aligned}&u=0\\&v_g=0\\&T=T_w\\&\rho_l=\rho_{lw}\end{aligned}\right\}\Rightarrow v_w=\frac{\rho_g+\rho_v}{\rho_g}D\frac{\partial}{\partial y}\left(\frac{\rho_g}{\rho_g+\rho_v}\right)$$

ρ_{lw} is unknown. For laminar boundary layers Hijikata and Mori's value of ρ_{lw} is used; for turbulent boundary layers, ρ_{lw} is obtained by successive approximations.

—for $y\to\infty$

$$u\to u_\infty$$
$$T\to T_\infty$$
$$\rho_l\to 0.$$

When the stream function Ψ and the Prandtl and Schmidt numbers are introduced in the above system, three partial differential equations remain; they are solved by using a finite-difference scheme based on the general method of Patankar and Spalding [3]. As it is a step-by-step method, initial profiles of velocity, temperature and concentration are needed:

—for laminar boundary layers, Blasius' profile is chosen;
—for turbulent boundary layers, the empirical approximation of Coles' law of the wake [4] is used.

In both cases, the initial energy and concentration profiles are deduced from the velocity profile by an analogy of the Crocco type, i.e.

$$\frac{h-h_w}{h_\infty-h_w}=\frac{u}{u_\infty}\qquad\frac{(\rho_g/\rho)-(\rho_g/\rho)_w}{(\rho_g/\rho)_\infty-(\rho_g/\rho)_w}=\frac{u}{u_\infty}.$$

However, for a turbulent boundary layer, some differences with the laminar one must be emphasized:

—u, v, h are replaced by their mean values $\bar{u}, \bar{v}, \bar{h}$;
—the fluctuation terms are introduced in the exchange parameters.

So, an 'effective' transfer parameter is determined as the sum of the laminar and turbulent contributions. Hence, the effective shearing stress τ_w can be written as:

$$\tau_w=(\mu_{lam}+\mu_{turb})\frac{\partial\bar{u}}{\partial y}\bigg|_w=\mu_{eff}\frac{\partial\bar{u}}{\partial y}\bigg|_w$$

where:

$$\mu_{turb}\frac{\partial\bar{u}}{\partial y}\bigg|_w=-\overline{(\rho v)'u'}=\rho l^2\left(\frac{\partial\bar{u}}{\partial y}\right)^2$$

which is the classical Prandtl mixing length hypothesis. The polynomial approximation of the mixing length l is due to Pletcher [5]; this approximation allows a smooth junction between the region of the vicinity of the wall where the laminar and turbulent contributions are of the same order of magnitude and the outer part of the boundary layer where l is assumed uniform and proportional to the boundary-layer thickness δ. When mass transfer occurs at the wall as in the present situation, the constant A of the Van Driest exponential damping factor must be modified by the introduction of the transverse velocity at the wall v_w according to [6].

The effective Prandtl and Schmidt numbers are assumed constant through the boundary layer and equal to 0.86 and 0.6, respectively; in the laminar case, $Pr=0.7$ and $Sc=0.6$.

With these hypothesis and an arbitrary value of ρ_{lw}, the calculation can yield, for each wall temperature, the

dynamic, thermal and concentration fields in the whole boundary layer when the physical properties of the mixture (pressure, velocity and temperature of the stream) are known. The good ρ_{lw} value is obtained by successive computer runs until the velocity, temperature and concentration profiles remain smooth in the whole field; the initial value was guessed from the laminar one. All the details of the numerical routine will be given in [7].

4. RESULTS

As was already noted in Section 2, direct measurements of heat transfer were not sufficiently accurate at least in laminar flow; measured and calculated temperature profiles should be first compared. For this purpose, let us point out that, in laminar and turbulent boundary layers, the location of the fictitious leading edge is not known; the abscissa at which the comparison would be done must be first determined. The dynamic boundary-layer thickness δ is calculated from the measured velocity profile, and the comparison with the numerical profile must be done at the abscissa where this thickness has the same value.

Then, if the agreement is good, heat transfer can be determined. Convective heat transfer due to the temperature difference between the wall and the free stream, called sensible heat transfer $\dot{q}_s$ is proportional to the temperature gradient at the wall and cannot be experimentally determined with sufficient accuracy. This gradient is then calculated; however, the most important part of heat transfer is due to the mass steam flux $\rho_v v_v$ which condenses on the cold wall. This condensation releases latent heat which is proportional to the latent heat coefficient (for steam, $L \simeq 2 \times 10^6$ J kg^{-1} K^{-1}). The total heat flux $\dot{q}_t$ is obtained by the addition of these two contributions; the latter can be up to 100 times greater than the former for a turbulent boundary layer with $T_\infty = 90°C$ and $\Delta T = 5°C$. Therefore, the total heat transfer is very closely related to mass transfer:

$$\dot{q}_t = \dot{q}_s + L(\rho_v v_v)_w$$

$$\dot{q}_t \simeq L(\rho_v v_v)_w.$$

Now, the steam mass flux at the wall is related to the diffusional velocity, itself a function of the temperature gradient; actually, the boundary condition $v_g|_w = 0$ yields a first relation between v_w and the diffusional velocity. A second relation is provided by equation (6) written for v_v:

$$v_v = v + \frac{\rho_g + \rho_v}{\rho_v} D \frac{\partial}{\partial y}\left(\frac{\rho_g}{\rho_g + \rho_v}\right).$$

These two relations yield:

$$v_v|_w = \left[\frac{(\rho_g + \rho_v)^2}{\rho_g \rho_v} D \frac{\partial}{\partial y}\left(\frac{\rho_g}{\rho_g + \rho_v}\right)\right]_w.$$

Then, as the gaseous components are assumed to be perfect, the $\rho_g/(\rho_g + \rho_v)$ gradient is directly related to the partial pressure gradient dp_v/dT multiplied by the temperature gradient dT/dy.

Therefore, the mass flux of steam and the total heat transfer are known as soon as the temperature gradient at the wall is known. The heat and mass transfer have been found again by an integral method based upon film theory [8].

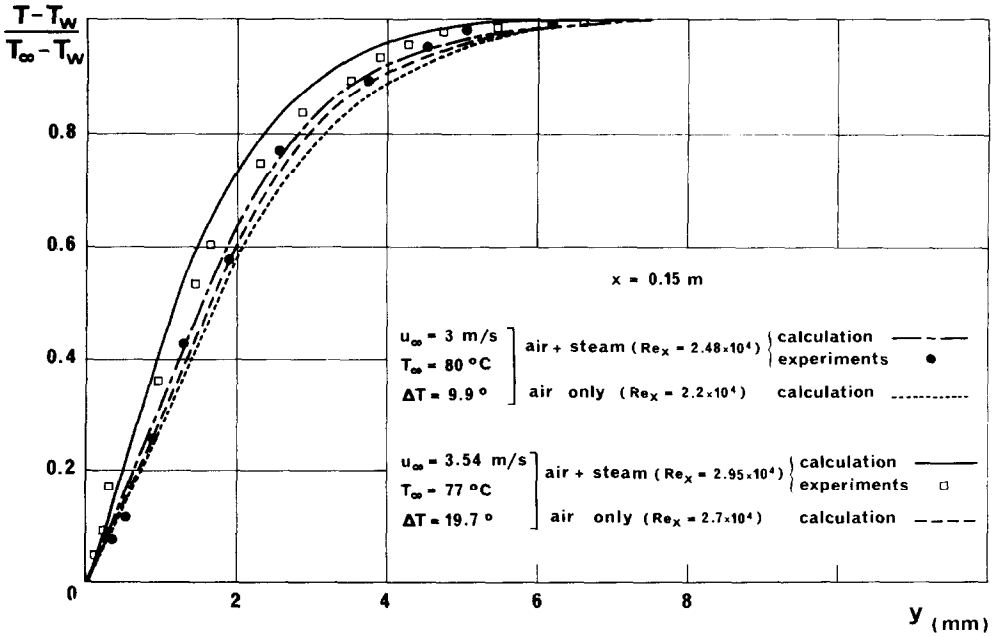

FIG. 1. Dimensionless temperature profiles in laminar boundary layer at $x = 0.15$ m.

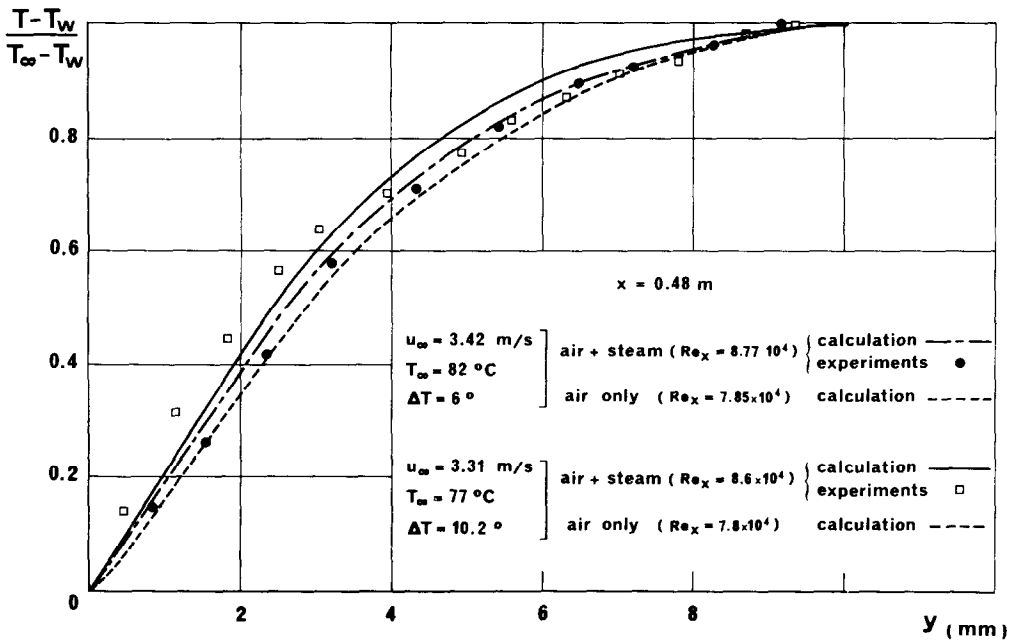

FIG. 2. Dimensionless temperature profiles in laminar boundary layer at $x = 0.48$ m.

4.1. *Laminar boundary layer*

In the laminar case the following results are obtained. Figures 1 and 2 show several cases of measured and calculated dimensionless temperature profiles: the agreement is good. From these two figures the influence of condensation on temperature profiles is obvious: the sensible heat transfer $\dot{q}_s$ is proportional to the slope of these profiles at the wall; and the temperature difference, $\Delta T = T_\infty - T_w$, is seen to be an influential factor on sensible heat transfer $\dot{q}_s$.

Since the numerical calculations and experiments are in agreement, various external and wall temperatures may be imposed in computation and conclusions may be deduced on heat and mass transfer. So, the external temperature T_∞ has been taken equal to 30°–40°C up to 90°C while the temperature difference varied between 0° and 30°C. Figure 3 shows the evolution of $\dot{q}_s/\dot{q}_{air}$ for a scale of T_∞ values; $\dot{q}_{air}$ is the heat flux in the case of forced convective air stream without steam. The improvement due to condensation, for only the part of

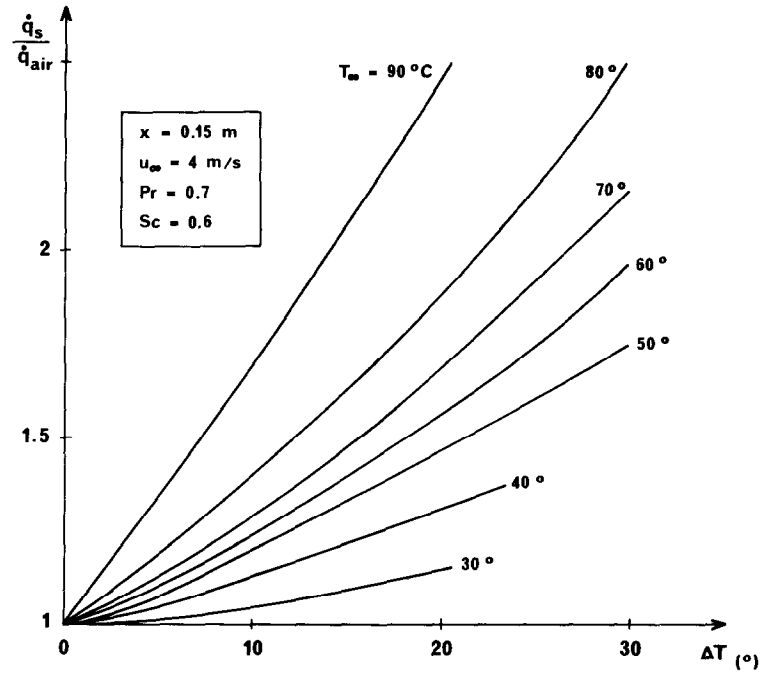

FIG. 3. Evolution of sensible heat transfer vs ΔT for various T_∞ (laminar boundary layer).

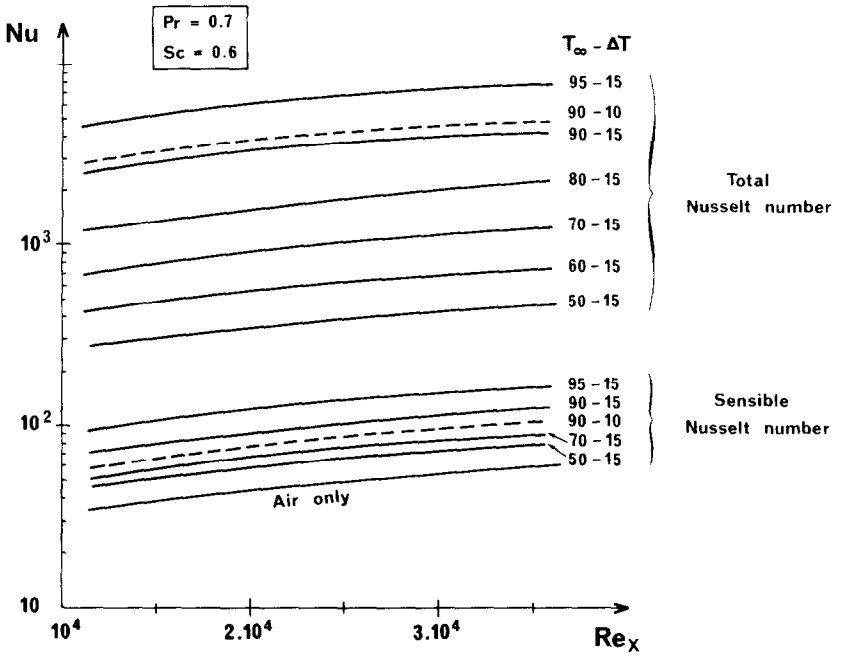

FIG. 4. Variation of Nusselt number vs Re_x for various conditions of temperature (laminar boundary layer).

sensible heat flux, is obvious and can be evaluated. Of course, sensible heat flux increases both with T_∞ and with ΔT [9].

The variation of Nusselt number for various temperatures is presented in Fig. 4. Let us define the 'sensible' Nusselt number as the Nusselt number which corresponds to sensible heat transfer only; 'total' Nusselt number takes into account the release of steam latent heat due to condensation. In this family of curves it should be noted that, for given ΔT and Re, the total Nusselt number is an increasing function of T_∞; however, for a given stream temperature, total Nusselt number is a decreasing function of ΔT. This surprising behavior can be explained by the fact that the Nusselt number varies in direct ratio of $\dot{m}_w/\Delta T$ for given stream conditions, and that ΔT decreases more quickly than $\dot{m}_w$. This is not the case for the sensible Nusselt number.

In Fig. 5 the $\dot{m}_w/\rho_\infty u_\infty$ ratio vs ΔT is plotted for various T_∞.

A comparison is shown in Fig. 6 between Hijikata and Mori's curves (in broken lines) and the present results. The agreement is good especially when ΔT is lower than 20°C.

4.2. *Turbulent boundary layer*

As in laminar boundary layers, a comparison between measured and calculated temperature profiles is first made in Fig. 7 where both experimental points and calculated profiles are plotted.

The dimensionless temperature profiles for dry air are calculated for the same main flow conditions. Sensible heat transfer is clearly improved by condensation; however, in all cases, the experimental points are seen to be distinctly above the calculated ones. This may be explained by the fact that some assumptions of the calculation could not be fulfilled experimentally [10]; for example:

- —The calculations were performed assuming a zero rate of preturbulence in the wind tunnel, while this rate is around 0.5% with a dry air flow and is obviously increased in the presence of air–steam mixture. Kestin *et al.* [11] showed that preturbulence influences heat transfer much more than velocity. This explains why such discrepancies did not appear in the velocity profiles.
- —The experimental evaluation of the boundary-layer thickness is not accurate and a small error on this thickness can lead to an important difference on the fictitious abscissa which is chosen in the calculations.
- —For steam–air flow, since no turbulent model could be found, a classical model for air only has been used; however, the choice of a turbulent model is quite arbitrary. Some authors have studied the influence of these various models on the results [12].
- —If the presence of a very thin film of plaster and water on the wall is taken into account, the experimental points are lowered especially in the vicinity of the wall. These corrected values, displayed in Fig. 7, are closer to the calculated ones.

In spite of these small discrepancies between the measured and calculated values, the sensible heat flux density at the wall can be deduced from the slope of the calculated temperature profiles. Hence, when this calculation is applied to other flow temperatures, the sensible heat flux at the wall can be predicted and, as in laminar boundary layers the total heat flux and, therefore, the total Nusselt number can be evaluated.

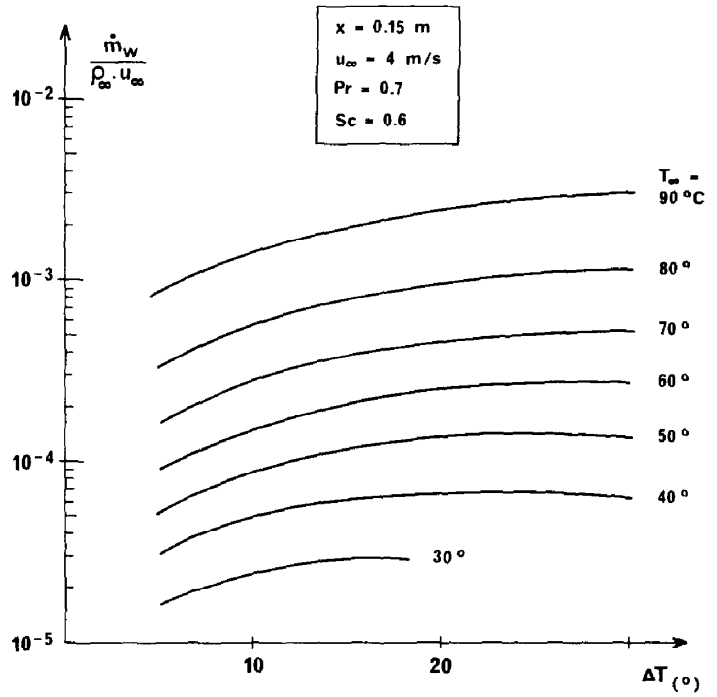

FIG. 5. Evolution of mass transfer at the wall vs ΔT for various T_∞ (laminar boundary layer).

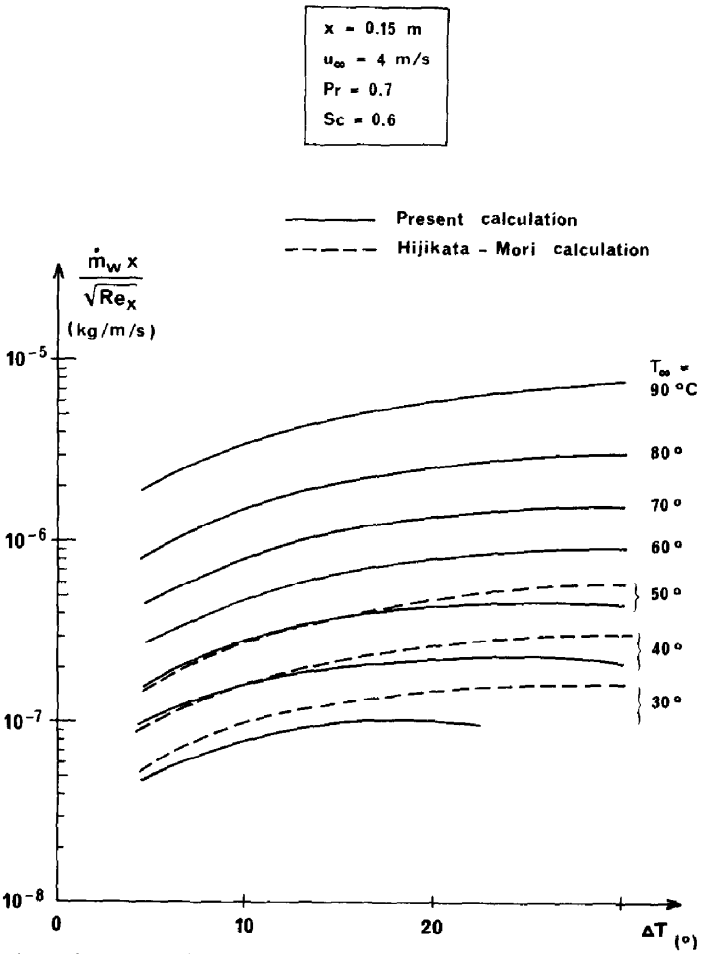

FIG. 6. Comparison of mass transfer between Hijikata and Mori's results and the present ones (laminar boundary layer).

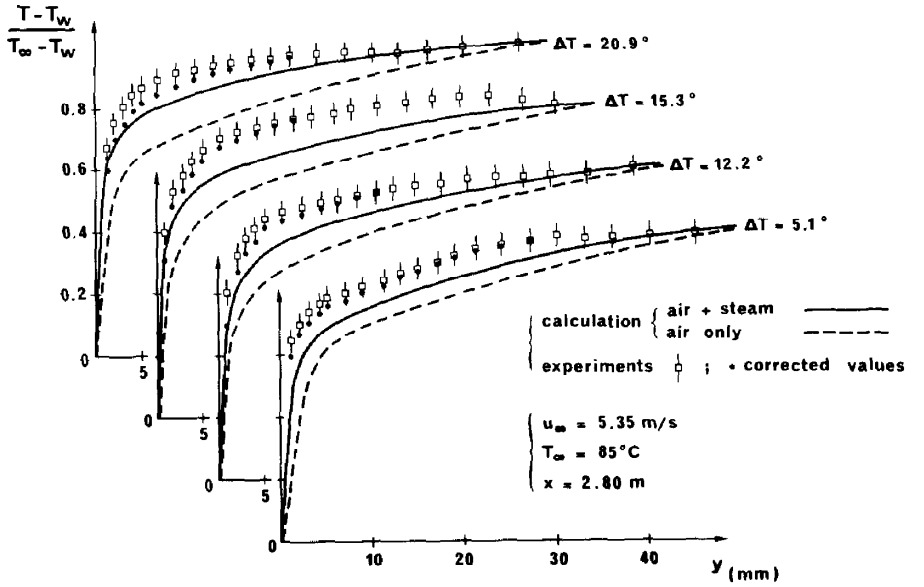

FIG. 7. Dimensionless temperature profiles in turbulent boundary layer.

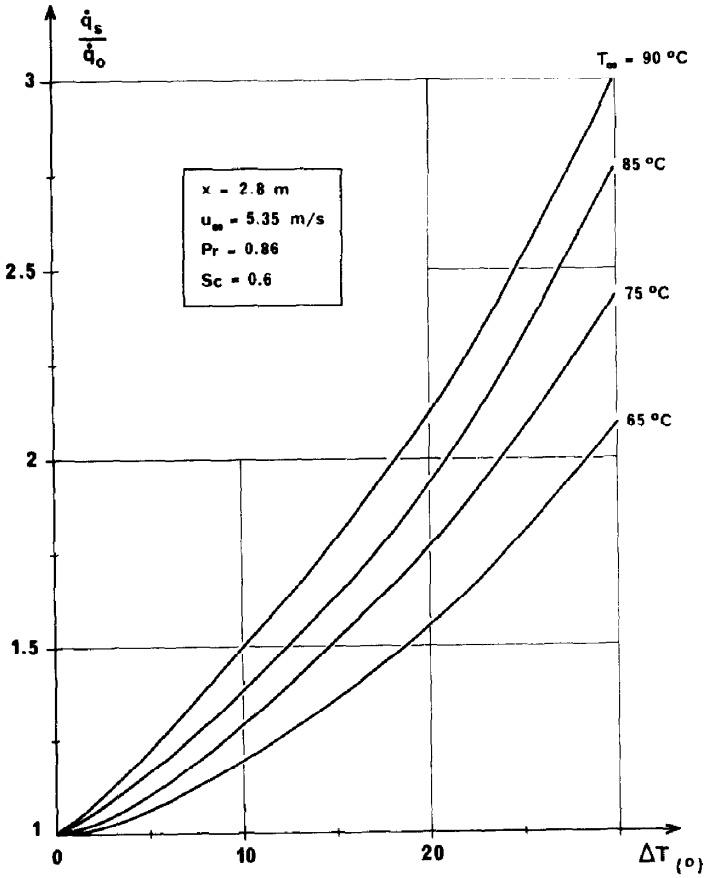

FIG. 8. Evolution of sensible heat transfer vs ΔT for various T_∞ (turbulent boundary layer).

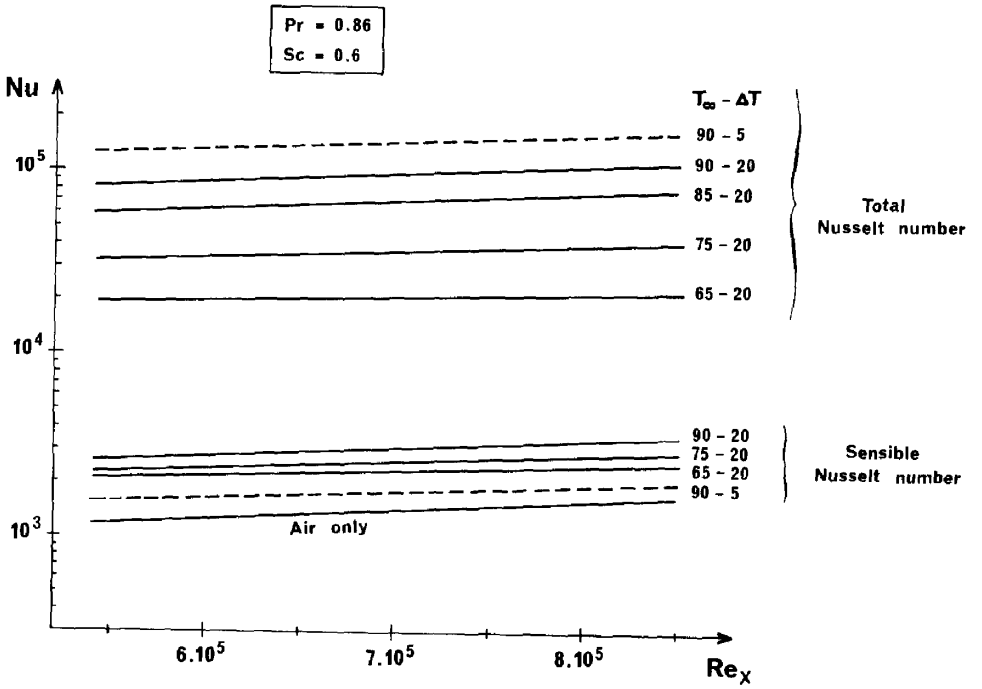

FIG. 9. Variation of Nusselt number vs Re_x for various conditions of temperature (turbulent boundary layer).

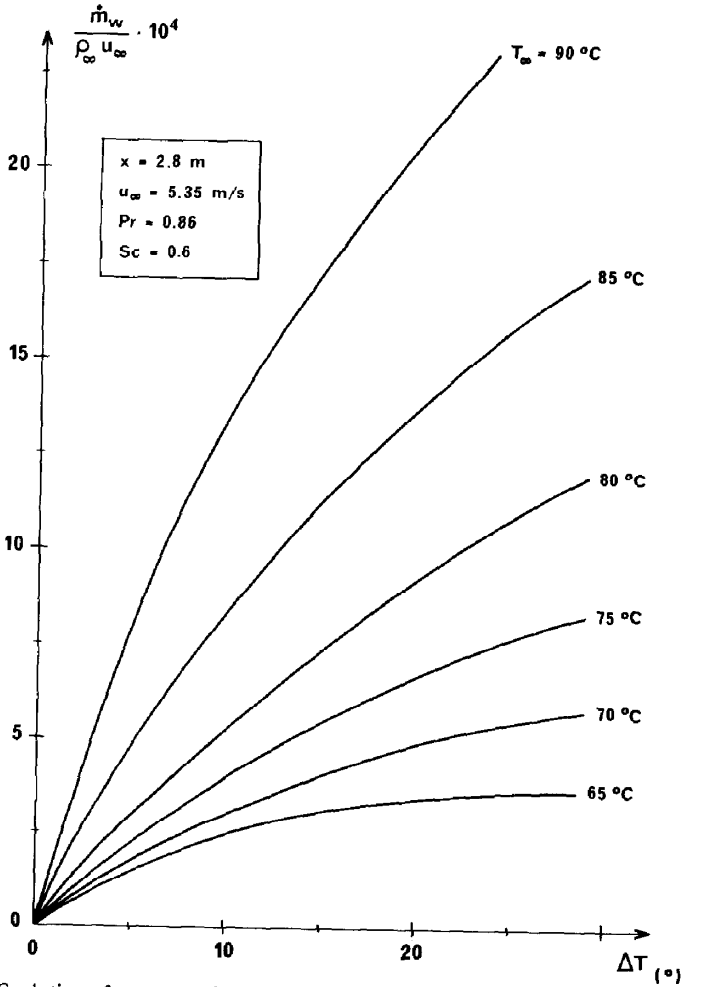

FIG. 10. Evolution of mass transfer at the wall vs ΔT for various T_∞ (turbulent boundary layer).

The $\dot{q}_s/\dot{q}_0$ variations are shown in Fig. 8, where $\dot{q}_0$ is the sensible heat transfer which would occur in the fictitious steam–air flow with a temperature gradient and no condensation. The same shape as in laminar boundary layer for $\dot{q}_s/\dot{q}_{air}$ (Fig. 3) is found.

Nusselt number vs Reynolds number curves are presented in Fig. 9. The improvement in heat transfer provided by condensation is clearly shown. For example, when $T_\infty = 90°C$ and $\Delta T = 20°C$, the sensible Nusselt number is seen to be about three times the value for air only and the total Nusselt number is seen to be 33 times the sensible Nusselt number.

As for the heat transfer, the mass flux density at the wall has been calculated for these various cases and results are presented in Fig. 10. It should be noticed that, for a same ΔT, the amount of liquid collected is more than three times its value when the flow temperature varies from 75° to 90°C, while the amount of steam present in the saturated mixture is only hardly doubled:

$$\rho_v\,(75°C) = 0.24\ \text{kg m}^{-3}$$

$$\rho_v\,(90°C) = 0.42\ \text{kg m}^{-3}.$$

This means that, when the external temperature increases, the ratio between the transverse flux of steam towards the wall and the longitudinal flux of steam carried away in the boundary layer, increases.

5. CONCLUDING REMARKS

Let us list our major results obtained for laminar and turbulent boundary layers with condensation:

- Some latent heat is produced by the phase change in a boundary layer; an important heat transfer is induced, which is much larger than for a dry air flow. This increased heat transfer and the mass flux at the wall can be predicted.
- A better heat exchange is obtained for a larger free-stream temperature and a larger difference of temperature between the wall and the free stream. However, since the number of droplets increases with this temperature difference, the model may not be valid anymore.
- As the latent heat of steam is large, the sensible heat flux is only a negligible part of the total heat flux; hence, heat and mass transfer are nearly proportional and are sensitive functions of the transverse velocity at the wall.

The present calculation can be easily applied to saturated mixing flows other than air and steam for a laminar boundary layer. Only the physical characteristics of the two components of the mixture, and the relation between the partial pressure of the studied vapor and the local temperature need to be known.

For a turbulent boundary layer, the calculations are valid if the effective exchange coefficients vary in a similar manner to the air coefficients.

The efficiency of condensation in heat exchangers is demonstrated; it suggests further technological studies of these devices.

REFERENCES

1. E. M. Sparrow, W. J. Minkowycz and M. Saddy, Forced convection condensation in the presence of non-condensable and interfacial resistance, *Int. J. Heat Mass Transfer* **10**, 1829–1845 (1967).
2. K. Hijikata and Y. Mori, Forced convective heat transfer of a gas with condensing vapour around a flat plate, *Heat Transfer–Jap. Res.* **2**, 81–101 (1973).
3. S. V. Patankar and D. B. Spalding, *Heat and Mass Transfer in Boundary Layers*, 2nd edn. Intertext, London (1970).
4. D. Coles, The law of the wake in turbulent boundary layer, *J. Fluid Mech.* **1**, 191–226 (1956).
5. R. H. Pletcher, On a finite-difference solution for the constant-property boundary layer, *A.I.A.A. Jl* **7**, 305–311 (1969).
6. F. Legay-Désesquelles, Etude théorique et expérimentale du transfert de chaleur et de masse dans une couche limite incompressible avec condensation sur une plaque plane. Thèse de Doct. d'Etat, Paris (1984).
7. F. Legay-Désesquelles et B. Prunet-Foch, Calcul des caractéristiques d'une couche limite incompressible avec condensation ou aspiration sur une plaque plane, Laboratoire d'Aérothermique R 85-3 (1985).
8. G. B. Diep, Transfert de chaleur et de masse par condensation dans une couche limite turbulente incompressible sur une plaque plane à faible niveau d'échange, *C.r. Acad. Sci. Paris* **296**, 1143–1146 (1983).
9. J. J. Bernard, G. B. Diep, F. Legay-Désesquelles et B. Prunet-Foch, Transfert thermique avec changement de phase dans une couche limite laminaire incompressible, *6th Int. Heat Transfer Conference*, Toronto, Vol. 2, pp. 335–339 (1978).
10. F. Legay-Désesquelles, B. Prunet-Foch and G. B. Diep, Heat and mass transfer in a low speed turbulent boundary layer with condensation, *7th Int. Heat Transfer Conference*, Munich, Vol. 6, pp. 123–127 (1982).
11. J. Kestin, P. F. Maeder and H. E. Wang, Influence of turbulence on the transfer of heat from plates with and without a pressure gradient, *Int. J. Heat Mass Transfer* **3**, 143–154 (1961).
12. W. P. Jones and U. Renz, Condensation from a turbulent stream onto a vertical surface, *Int. J. Heat Mass Transfer* **17**, 1019–1028 (1974).

TRANSFERT DE CHALEUR ET DE MASSE DANS UNE COUCHE LIMITE LAMINAIRE ET TURBULENTE AVEC CONDENSATION, LE LONG D'UNE PLAQUE PLANE

Résumé—L'étude expérimentale et numérique présentée ici porte sur le transfert de chaleur et de masse dans une couche limite incompressible avec condensation sur une plaque plane. L'écoulement, à la pression atmosphérique, est constitué d'un mélange d'air saturé en vapeur d'eau ; sa vitesse est inférieure à 6 m s^{-1}, le nombre de Reynolds rapporté à l'abscisse le long de la plaque est de l'ordre de 10^4 à 10^5 pour la couche limite laminaire, et de 3×10^5 à 10^6 pour la couche limite turbulente. L'écart de température entre l'écoulement principal et la paroi refroidie reste inférieur à 20°C. Une méthode par différences finies est employée pour calculer les champs de vitesse, de température et de concentration. Les résultats obtenus numériquement sont en bon accord avec ceux fournis par l'expérience. Ainsi, à partir de ce calcul, les transferts de chaleur et de masse peuvent être prévus, pour d'autres conditions.

WÄRME- UND STOFFÜBERTRAGUNG BEI DER KONDENSATION IN LAMINAREN UND TURBULENTEN GRENZSCHICHTEN AN EINER EBENEN PLATTE

Zusammenfassung—Eine experimentelle und numerische Untersuchung des Wärme- und Stoffüberganges bei der Kondensation in inkompressiblen Grenzschichten an einer ebenen Platte wird dargestellt. Eine Luft-Dampf-Strömung bei Atmosphärendruck ist gesättigt; ihre Geschwindigkeit ist kleiner als 6 m s^{-1}; der Bereich der Reynoldszahl—gebildet mit der Lauflänge—erstreckt sich von 10^4 bis 10^5 für die laminare Grenzschicht und von 3×10^5 bis 10^6 für die turbulente. Die Temperatur-Differenz zwischen der Hauptströmung und der Wand ist kleiner als 20 K. Mit Hilfe eines Finite-Differenzen-Verfahrens werden Geschwindigkeits-, Temperatur- und Konzentrationsverteilungen berechnet. Die numerischen und experimentellen Ergebnisse stimmen für die laminare und die turbulente Grenzschicht gut überein.

ТЕПЛО- И МАССОПЕРЕНОС ПРИ КОНДЕНСАЦИИ В ЛАМИНАРНОМ И ТУРБУЛЕНТНОМ ПОГРАНИЧНЫХ СЛОЯХ НА ПЛОСКОЙ ПЛАСТИНЕ

Аннотация—Проведено экспериментальное и численное исследование тепло-и массопереноса в пограничном слое несжимаемой жидкости при конденсации на плоской пластине. Исследуется обтекание пластины смесью воздуха с насыщенным паром при атмосферном давлении. Скорость потока меньше 6 м/с при числах Рейнольдса, рассчитанных по направленной вдоль пластины абсциссе, в диапазоне 10^4–10^5 для ламинарного пограничного слоя и 3×10^5–10^6—для турбулентного слоя. Разность температур между основным потоком и холодной стенкой не превышает 20°C. Поля скорости, температуры и концентрации рассчитываются методом конечных разностей; численные результаты хорошо согласуются с экспериментальными данными для ламинарного и турбулентного пограничных слоев.